Bending Characteristics of Asymmetric SOI Polarization Rotators

Henghua Deng, *Member, IEEE*, David O. Yevick, *Fellow, IEEE*, and Sujeet K. Chaudhuri, *Senior Member, IEEE*

***Abstract*—We examine polarization conversion and radiation and transition losses in bending slanted-angle silicon-on-insulator polarization rotators.**

***Index Terms*—Beam propagation method, bending analysis, finite-element method (FEM), polarization rotator (PR), silicon-on-insulator (SOI).**

I. Introduction

INTEGRATED polarization rotators (PRs) employ material anisotropy or geometric asymmetry to couple light from transverse-electric (TE) to transverse-magnetic (TM) polarization states. Of these, asymmetrically loaded periodic [1], [2] or single-section slanted-angle [3], [4] passive devices are particularly compact and simple to fabricate. However, as demonstrated in InGaAsP, full polarization rotation can be achieved with low insertion loss in bent waveguides [5]. A microring resonator realization was similarly performed in [6]. Theoretical studies of bent-waveguide structures employ a conformal transformation to map the refractive index profile onto an equivalent straight waveguide [7]–[9]. Analyses based on the finite-difference and coupled mode procedures are given in [9] while finite-element field propagation programs were employed in [10].

In this letter, we apply a full vectorial finite-element method (FEM) to determine the effect of bending on the asymmetric slanted-angle passive silicon-on-insulator (SOI) PR structures discussed in [3], [4]. Our analysis demonstrates that such waveguides are relatively insensitive to bending when the slanted face is positioned at the outer radius of the bend.

II. Waveguide Geometry

The SOI polarization rotating waveguide that we will examine is depicted in Fig. 1, where the slanted facet is etched completely down to the insulating oxide layer along the (111) crystal plane yielding an angle of 54.736° with respect to the horizontal direction. The Si and SiO_2 refractive indexes are $n_1 = 3.48$ and $n_2 = 1.45$, respectively, while the rib waveguide height, width, and the thickness of the outer slab are $H = 2.8\ \mu$m, $W = 2.7\ \mu$m, and $h = 1\ \mu$m, respectively.

Manuscript received February 9, 2005; revised May 11, 2005. This work was supported by the Canadian Institute for Photonic Innovations (CIPI), and by the Natural Science and Engineering Research Council of Canada (NSERC).

H. Deng and S. K. Chaudhuri are with the Department of Electrical and Computer Engineering, University of Waterloo, Waterloo, ON N2L 3G1, Canada (e-mail: hdeng@uwaterloo.ca; sujeet@maxwell.uwaterloo.ca).

D. O. Yevick is with the Department of Physics, University of Waterloo, Waterloo, ON N2L 3G1, Canada (e-mail: yevick@uwaterloo.ca).

Digital Object Identifier 10.1109/LPT.2005.856334

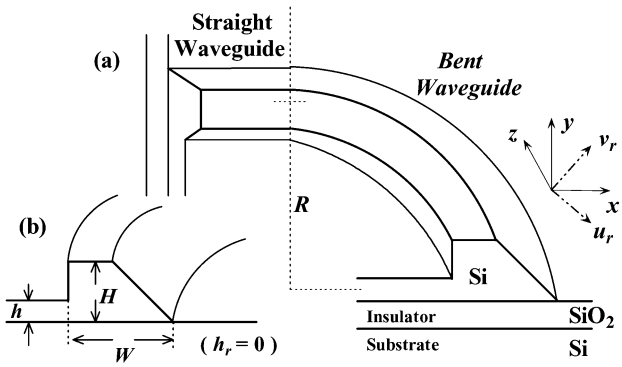


Fig. 1. Bend orientations for the slanted-angle SOI PR: (a) slanted facet at outer bend radius; and (b) vertical facet at outer bend radius.

For these parameter values, the TE and TM components of the two lowest-order modes have comparable amplitudes so that the optical-axis, denoted by (u_r, v_r), is rotated by $\varphi = 46.24°$. The maximum polarization conversion efficiency [3] is PC $= 99.81\%$ so that a TE polarized input is nearly completely converted to a TM field after a half-beat length [3] $L_\pi = \pi/(\beta_1 - \beta_2) = 490.08\ \mu$m. Obviously, because of the asymmetric geometry, the two possible bending orientations illustrated in Fig. 1(a) and (b) yield physically different results.

III. Computational Method

To analyze the bent SOI slanted-angle waveguide, we employ the vectorial wave equation for the magnetic field

$$\nabla \times \left(\frac{1}{n^2}[s]^{-1} \nabla \times \mathbf{H} \right) - k_0^2 [s] \mathbb{H} = 0 \tag{1}$$

where $\boldsymbol{H}, k_0$, and n denote the magnetic field, vacuum wave number, and refractive index, respectively. Near the boundaries of the computational grid, we employ an anisotropic perfectly matched layer (PML) such that $[s]$ is a 3×3 diagonal matrix insider the PML layer [11] and the identity matrix elsewhere.

Applying the Crank–Nicholson approach to the above equation leads to a propagation procedure of the form

$$([K] - k_0^2 n_0^2 [M])\{H\} = 2jk_0 n_0 [M] \frac{d\{H\}}{dz}. \tag{2}$$

Since the standard eigenmode equation is obtained by omitting the z-derivative term, for the FEM with hybrid edge/nodal mixed triangular elements, the matrices $[K]$ and $[M]$ are given in [11]. Bent waveguides are then normally modeled by adding the term $n_t(x, y) = n(x, y)(1 + x/R)$ [7] to the index distribution. Our calculations employ adaptive mesh generation starting from the nonuniform mesh of Fig. 2.

1041-1135/$20.00 © 2005 IEEE

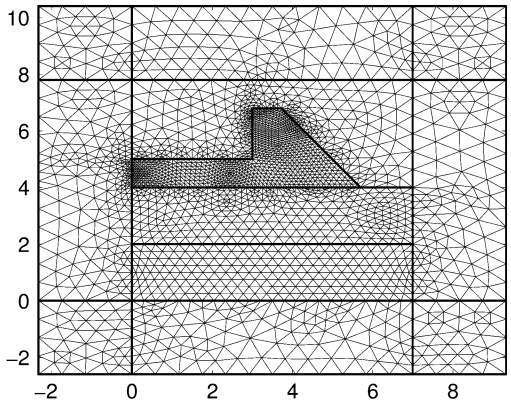


Fig. 2. Nonuniform grid employed in the finite-element calculations for the waveguide surrounded by anisotropic PML layers (units in micrometers).

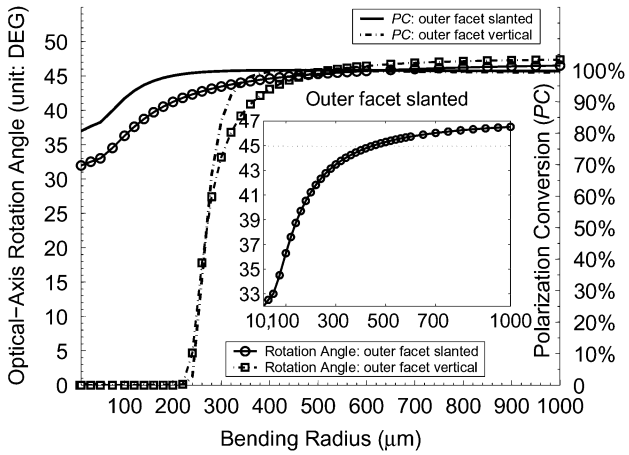


Fig. 3. Optical axis rotation angle φ and polarization conversion efficiency as a function of bending radius.

IV. Polarization Conversion

We first consider the influence of waveguide bending on the optical axis orientation. In particular, Fig. 3 displays the optical axis rotation angle φ as a function of the bending radius. As expected, the result depends critically on whether the sloped or the vertical waveguide facet forms the outer radius of the bend. In the first case, we adjusted the waveguide parameters to yield a $\varphi = 45°$ rotation-angle at the half-beat length $L_\pi = 400\ \mu$m and bending radius $R = 450\ \mu$m. Then, at $R = 200\ \mu$m, the half-beat length is $L_\pi = 317.79\ \mu$m, corresponding to a 91° bend. After 90°, the optical axis rotation is $\varphi = 41.22°$ yielding a 98.27% TE $\leftrightarrow$ TM conversion efficiency. Further decreasing the bending radius to $100\ \mu$m still results in a maximum conversion efficiency of 91.04% for a length of L_π. In contrast, if the vertical facet is situated at the outer radius, the optical axis rotation decreases rapidly with bending radius for $R < 400\ \mu$m. When a 45° optical axis rotation is attained at $R = 470\ \mu$m for this bend orientation, we find $L_\pi = 628\ \mu$m. For the radius of curvature $R = 264.76\ \mu$m at which the half-beat length $L_\pi = 415.88\ \mu$m coincides with a 90° bend, the optical axis rotation and polarization conversion are approximately 18° and 34%.

To understand the behavior of the bent waveguides, consider the $R = 50\ \mu$m magnetic field amplitudes of Fig. 4 (the corresponding field distribution in the straight waveguide is illustrated in [3], [4]). When the slanted facet describes the outer bending radius, the field shifts toward the facet, changing the field patterns and propagation constants of both waveguide modes by nearly the same amount. Hence, the bent waveguide still functions as a single-section polarization converter [3]. However, if the vertical facet is located at the outer bending radius, the electromagnetic field instead radiates into the slab layer. As shown in the right side of Fig. 4, for $R = 50\ \mu$m, the first lowest-order mode is a radiating quasi-TM mode for which H_x is the nondominant component. Accordingly, at small bending radii, acceptable polarization conversion is only achieved with a sloped sidewall outer facet.

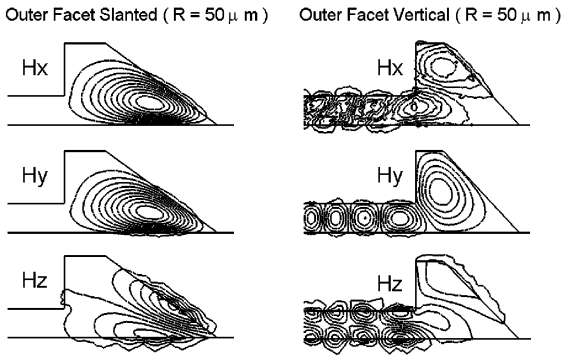


Fig. 4. Magnetic field distribution of the first lowest-order mode in a bent slanted-angle SOI waveguide with a $R = 50\ \mu$m radius of curvature. In the three diagrams on the left, the slanted facet constitutes the outer radius of the bend, while in the right diagrams, the vertical facet is instead the outer radius.

V. Waveguide Losses

Losses in optical waveguides are divided into stead-state bending loss and transition loss. The first of these can be calculated from the imaginary part of the propagation constant, while the second results from the mismatch of the fundamental field distributions of the bent and straight waveguides and is, therefore, evaluated according to

$$L_T = 10\log_{10}\left[\frac{|\int\int \phi_s\phi_b^* dS|^2}{|\int\int \phi_s\phi_s^* dS| \cdot |\int\int \phi_b\phi_b^* dS|}\right] (\text{dB}) \quad (3)$$

where ϕ_s and ϕ_b are the lowest-order similarly polarized field distributions of the straight and bent waveguides, respectively.

In our waveguide structure, bends in which the vertical facet is located at the outer radius yield a large bending loss into the outer-slab waveguide for $R < 300\ \mu$m, as evident from Fig. 5. If, however, the slanted facet is on the outside of the bend, the field is displaced toward the slanted wall, suppressing radiation losses, as evident from Figs. 4 and 5.

We next display in Fig. 6 the transition loss as a function of bending radius induced by butt-coupling our slanted-angle SOI waveguide to straight input and output waveguides as in Fig. 1. Evidently, the transition loss increases rapidly if the vertical facet is located at the outer bending radius for $R < 260\ \mu$m (although in this case we are evaluating the overlap of the input field with the radiation field which generates a somewhat spurious result). If the slanted-angle facet instead is placed at the outer boundary, the transition loss remains less than 1 dB for

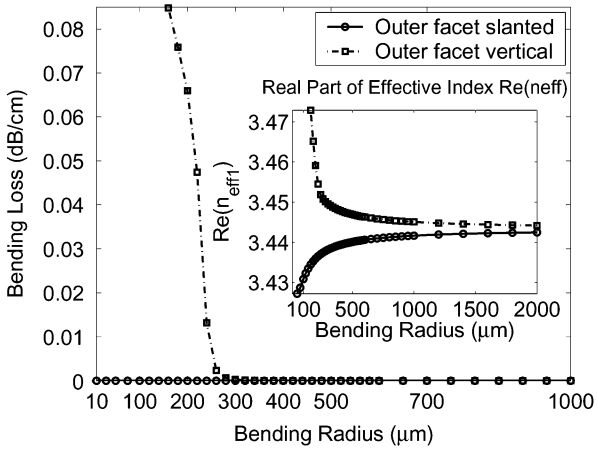


Fig. 5. Bending loss as a function of bending radius. The inset shows the variation of the real part of the effective index of the lowest-order fundamental mode.

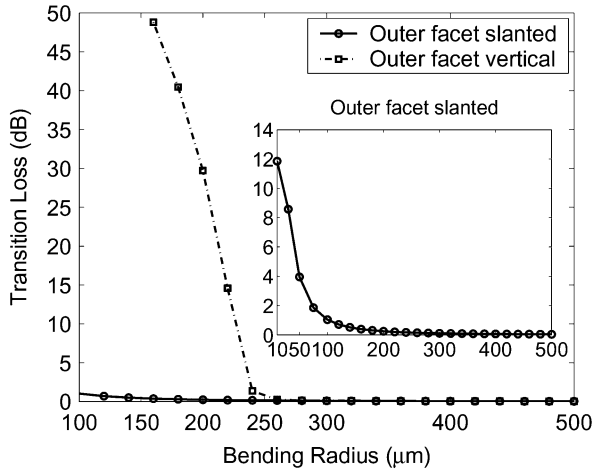


Fig. 6. Transition loss as a function of bending radius.

$R > 100$ μm, while for a 90° bend with $R = 200$ μm and $L_\pi = 317.79$ μm, the transition loss is only 0.24 dB.

VI. Conclusion

We have found that asymmetric SOI slanted-angle waveguides can exhibit a high degree of insensitivity to bending loss while maintaining a large coupling coefficient to external waveguides and fibers. Such bent waveguides can be employed to alter both the direction and the polarization of a propagating field, and could be utilized in many integrated optic components such as polarization-insensitive arrayed-waveguide gratings (AWGs). In this application, slanted-angle waveguides would replace a half-wave plate, which typically is associated with large (≈5 dB) coupling losses [12]. While bent waveguides with a constant slanted-angle [13], [14] are obviously difficult to fabricate, this difficulty could eventually be surmounted by, e.g., novel reactive-ion-etching techniques. Indeed, our general design rules [3] work for arbitrary slanted-angle and relax restrictions on fabrication requirements.

References

[1] Y. Shani, R. Alferness, T. Koch, U. Koren, M. Oron, B. I. Miller, and M. G. Young, "Polarization rotation in asymmetric periodic loaded rib waveguides," *Appl. Phys. Lett.*, vol. 59, no. 11, pp. 1278–1280, Sep. 1991.

[2] J. J. G. M. van der Tol *et al.*, "Realization of a short integrated optic passive polarization converter," *IEEE Photon. Technol. Lett.*, vol. 7, no. 8, pp. 893–895, Aug. 1995.

[3] H. Deng, D. O. Yevick, C. Brooks, and P. E. Jessop, "Design rules for slanted-angle polarization rotators," *J. Lightw. Technol.*, vol. 23, no. 1, pp. 432–445, Jan. 2005.

[4] ——, "Design procedures for slanted-angle SOI polarization rotators," in *OSA/IEEE Proc. Optical Fiber Communication Conf. (OFC 2004)*, Los Angles, CA, Feb. 22–27, 2004, Paper MF-41.

[5] C. van Dam *et al.*, "Novel compact polarization converters based on ultra short bends," *IEEE Photon. Technol. Lett.*, vol. 8, no. 10, pp. 1346–1348, Oct. 1996.

[6] B. E. Little and S. T. Chu, "Theory of polarization rotation and converqion in vertically coupled microsesonators," *IEEE Photon. Technol. Lett.*, vol. 12, no. 4, pp. 401–403, Apr. 2000.

[7] P. Danielsen and D. Yevick, "Propagating beam analysis of bent optical waveguides," *J. Opt. Commun.*, vol. 4, pp. 94–98, 1983.

[8] C. Vassallo, *Optical Waveguide Concepts*. Armesterdam, The Netherlands: Elsevier, 1991.

[9] W. W. Lui, C.-L. Xu, T. Hirono, K. Yokoyama, and W.-P. Huang, "Full-vectorial wave propagation in semiconductor optical bending waveguides and equivalent straight waveguide approximations," *J. Lightw. Technol.*, vol. 16, no. 5, pp. 910–914, May 1998.

[10] S. S. A. Obayya, B. M. A. Rahman, K. T. V. Grattan, and H. A. El-Mikati, "Beam propagation modeling of polarization rotation in deeply etched semiconductor bent waveguides," *IEEE Photon. Technol. Lett.*, vol. 13, no. 7, pp. 681–683, Jul. 2001.

[11] K. Saitoh and M. Koshiba, "Full-vectorial imaginary-distance beam propagation method based on a finited element scheme: Application to photonic crystal fibers," *IEEE J. Quantum Electron.*, vol. 38, no. 7, pp. 927–933, Jul. 2002.

[12] H. Takahashi, Y. Hibino, and I. Nishi, "Polarization-insensitive arrayed-waveguide grating wavelength multiplexer on silicon," *Opt. Lett.*, vol. 17, no. 7, pp. 499–501, Apr. 1992.

[13] R. J. Deri, A. Shahar, E. Colas, R. N. Thurston, W. J. Tomlinson, A. Yi-Yan, and M. Seto, "Single-mode semiconductor optical waveguides with large dimensions suitable for compact bend applications," *Appl. Phys. Lett.*, vol. 57, no. 23, pp. 2396–2398, Dec. 1990.

[14] S. Kitamura, H. Hatakeyama, T. Tamanuki, T. Sasaki, K. Komatsu, and M. Yamaguchi, "Angled-facet S-bend semiconductor optical amplifiers for high-gain and large-extinction ratio," *IEEE Photon. Technol. Lett.*, vol. 11, no. 7, pp. 788–790, Jul. 1999.